PNAS RESEARCH ARTICLE | EARTH, ATMOSPHERIC, AND PLANETARY SCIENCES
ENVIRONMENTAL SCIENCES OPEN ACCESS

Rising rates of wildfire building destruction in the conterminous United States

Amanda R. Carlson[a,1], Todd J. Hawbaker[a], Miranda H. Mockrin[b], Volker C. Radeloff[c], Lucas S. Bair[d], Michael D. Caggiano[e], James R. Meldrum[f], Patricia M. Alexandre[g], H. Anu Kramer[c], and Paul F. Steblein[h]

Affiliations are included on p. 8.

Edited by Janet Franklin, San Diego State University, San Diego, CA; received March 18, 2025; accepted November 13, 2025

Many regions of the world have seen an increase in highly destructive wildfires, driven by well-documented increases in burned area and growth of housing in the wildland–urban interface (WUI), which exposes more homes to fire. However, it is unclear whether wildfires are also becoming more destructive due to changes in wildfire behavior or in the development patterns of exposed communities. Here, we assessed trends in wildfire building exposure and destruction rates in the conterminous United States from 2002 to 2022. We mapped destroyed and surviving buildings within 100 m of all wildfires that destroyed 10 or more buildings (n = 362) and assessed trends relative to major ecoregions and vegetation types. We used logistic regression to assess relationships between destruction rates and landscape factors. We found that 10% of exposed buildings were destroyed in 2002–2012, but this percentage increased to 32% in 2013–2022. This increase was largely due to greater building exposure in evergreen forests in the northwestern United States, where exposed buildings were more than 3.4 times as likely to be destroyed as those in grass and shrublands. However, annual destruction rates also significantly increased in all other vegetation types and were correlated with development type, weather, and burn severity. These results indicate that increasing wildfire destruction in the United States has resulted not only from increased exposure but from rising rates of building destruction, potentially indicating more extreme wildfire behavior. This finding underscores the need to better understand how fuel management, community planning, and hardening buildings can reduce vulnerability.

wildland fire | building destruction | wildland–urban interface | global change | wildfire risk

Significance

Highly destructive wildfires are occurring more frequently across the globe, prompting debates over the causes for this increase and effective management responses. We investigated building destruction trends in the United States by mapping buildings that were exposed to and destroyed by wildfires over two decades. The proportion of exposed buildings that were destroyed more than tripled from 2002–2022, indicating that wildfires became more destructive in addition to burning more populated areas. This increase in destruction rate was linked to greater building exposure in forests, but destruction rates also increased in grass and shrublands and were influenced by weather, development type, and burn severity. Our findings suggest that diverse management approaches may be needed to reduce community vulnerability to wildfire disasters.

Highly destructive wildfires are occurring more frequently in many parts of the world (1). Many of the most destructive events in modern history have occurred since the mid-2010s, including the 2018 Camp fire in northern California, United States of America (>16,000 reported burned structures), the 2019–2020 Black Summer fires in southeastern Australia (>3,000 structures), the 2023 Lahaina fire in Hawaii, United States of America (>2,200 structures), and the 2025 Palisades and Eaton fires in Los Angeles, United States of America (>10,000 structures). Many of these events occurred in the western United States, where over 59,000 structures were destroyed by wildfires from 2010–2023 (2). Wildfires since 2015 have caused USD $136 billion in economic losses globally (3), as well as enormous insurance losses that resulted in loss of coverage for tens of thousands of homeowners (4). Destructive wildfires also have severe long-term economic impacts, disrupt communities, and have lasting effects on public health (5). Adapting to changing patterns of wildfire destruction and developing effective risk mitigation policies is, therefore, an important management concern.

Increasing wildfire building destruction may result from 1) increases in wildfire frequency and burned area, 2) growth of housing in the wildland–urban interface (WUI), where homes are most likely to be exposed to wildfires, or 3) more extreme wildfire behavior that makes suppression less effective. Global burned areas have decreased since the late 20th century but have increased specifically in high-latitude forests, particularly in western North America (6). The United States has experienced significant increases in wildfire burned area and average wildfire size since the 1980s as a result of lengthening fire seasons and greater frequency, duration, and severity of droughts (7–9). The footprint and number of homes in the WUI has also grown substantially in the United States, and this growth leads to more frequent wildfire ignition near homes and more homes exposed when wildfires occur (2, 10). Increases in burned area and housing growth in the WUI have contributed approximately equally to increases in home exposure within burned areas since 1990 (11, 12). At the same time, extreme fire weather and changes in fuel structure have potentially contributed to more extreme wildfire behavior. Fire suppression

The authors declare no competing interest.

This article is a PNAS Direct Submission.

[1]To whom correspondence may be addressed. Email: arcarlson@usgs.gov.

This article contains supporting information online at https://www.pnas.org/lookup/suppl/doi:10.1073/pnas.2505886122/-/DCSupplemental.

Published December 15, 2025.

during the 20th century has led to excess fuel build-up in many western US forests that were adapted to frequent burning, while the western United States has also experienced widespread forest die-offs from drought and insects since ca. 2000 (13–15). Rates of wildfire spread have increased in the western United States, and these fast-spreading fires are associated with high destruction (7, 16, 17). However, changes in the destructive potential of wildfires are less well-understood than changes in wildfire burn probability or increases in the number of vulnerable homes in the WUI.

Policy discussions about mitigating wildfire disasters often focus on fuels management and particularly on reducing forest fuels (18, 19). However, wildfires in different vegetation types may require different management approaches. A majority of burned area in the WUI in the United States is in grass and shrublands rather than forests (11, 20), and although grass and shrubland fuel management can help to reduce wildfire intensity near homes, destructive events in these landscapes are also strongly influenced by human-caused ignitions and high winds (10, 21). Fuel treatments in these landscapes may be less effective during extreme high winds and also require frequent maintenance to prevent regrowth by invasive species (22, 23). Management in grass and shrublands may therefore focus on reducing accidental ignitions (e.g., by burying power lines). In forests, mechanical thinning, prescribed burning, and fuel breaks are effective at reducing wildfire intensity in low-elevation dry forests that have been altered by past suppression (24). Suppression histories have had less significant effects in high-elevation, wet forests characterized as having "low-frequency, high-intensity" fire regimes, which are at risk of highly destructive events as a result of climate-driven increases in wildfire activity (25, 26). Fuel management in these ecosystems is challenging due to dense vegetation and steep terrain, and risk reduction may therefore focus instead on community preparedness. Determining which management strategies to prioritize requires consideration for which communities are at greatest risk of destruction, and how risk is affected by fuel type.

Reducing wildfire risk to communities may also involve making structures less susceptible to destruction. The WUI is where most homes are exposed to wildfires (27), but characteristics of homes and neighborhoods also influence the probability that buildings will be destroyed when wildfires occur. Broadly, the WUI is made up of two types: the intermix, where housing above a minimum density threshold (>6.17 houses per km^2) intermingles with wildland vegetation, and the interface, where housing abuts but does not intermingle with wildland vegetation (28). Building density and vegetation in the defensible space around buildings affect destruction probability, such that destruction rates are higher in lower-density areas with more surrounding vegetation (29–31). Factors such as building materials and construction age also influence probabilities of ignition and home-to-home flame spread (32, 33). Management strategies focused on reducing home-to-home flame transmission (e.g., building codes, homeowner outreach) may be as important for reducing destruction as strategies focused on fuel reductions to control wildfire behavior (34).

Understanding wildfire destruction patterns across the United States is important for developing effective wildfire risk mitigation policies, particularly with respect to rapid changes in burned area and wildfire behavior. Here, we evaluated 21st-century trends and predictors of building destruction rates, or numbers of buildings destroyed relative to numbers exposed, in the conterminous United States. Our evaluations were based on mapping locations of all exposed buildings within and adjacent to the perimeters of destructive fires (≥10 buildings destroyed; n = 362 fires) from 2002–2022 (see *Materials and Methods*; Fig. 1*A*; 31, 35–37). The final dataset included 73,534 destroyed buildings and an additional 1.70 million surviving buildings that were within 2.4 km of mapped wildfire perimeters, representing the approximate distance over which buildings can be ignited by embers (38). Spatially precise data building locations allowed us to assess destruction rates using consistent counts of exposed and destroyed buildings and to assess predictors of destruction in relation to vegetation and other landscape factors. We evaluated building destruction rates by dividing the number of destroyed buildings by the number of buildings that were "directly" exposed, i.e., within or <100 m outside the fire perimeter (n = 294,209; see *Materials and Methods*). Our aims were to 1) assess trends in numbers of exposed and destroyed buildings and destruction rates for the entire conterminous United States and by major ecoregions (38; Fig. 2*A*), 2) assess trends and relative destruction likelihood by major vegetation types, and 3) assess how destruction rates varied with vegetation cover, WUI types, building density, distance to high-severity burned area, final fire size, and weather. For objective 3), we used logistic regression to model destruction rates for clusters of buildings within wildfire events (i.e., groups of buildings within 1 km of one another; see *Materials and Methods*). Our results inform the likely causes of increasing building destruction in the United States and have broad implications for risk management.

Results

Rates of Wildfire Building Destruction Are Increasing Across the Conterminous UnitedStates. The number of destructive events, numbers of destroyed buildings, and rate of destruction increased dramatically in the conterminous United States from 2002 to 2022 (Fig. 1). During the first half of this period from 2002 to 2012, we mapped 119 events that destroyed 905 buildings per year, on average (std. dev.: 934), with an overall destruction rate of 10.1%. From 2013 to 2022, we mapped nearly twice as many destructive events (n = 243). There was a nearly seven-fold increase in the annual number of destroyed buildings (6,239 ± 6,974) and a three-fold increase in the destruction rate (31.9%; Fig. 1 *B* and *C*). Notably, the annual trend in buildings exposed to destructive wildfires was positive (517 buildings/year) but only weakly significant (P = 0.085; Table 1), as building exposure in 2003 and 2007 was comparable to more recent highly destructive years in 2017, 2018, and 2020 (Fig. 1*B*). In contrast, the number of destroyed buildings significantly increased at a rate of 208 buildings/year, or by 23% of the mean number of destroyed buildings from 2002 to 2012 (P = 0.009; Table 1 and *SI Appendix*, Table S1). It is unclear whether this increase in destruction rate was caused by more extreme wildfire behavior, less effective suppression, changes in the vulnerability of exposed communities, or other factors, but it is concerning given the increases in wildfire burned area and development in the WUI.

We considered whether our trend assessments were affected by potential undercounting of destroyed buildings in earlier fires. Building maps based on older aerial imagery were subject to greater uncertainty due to coarser image resolution (1 to 3 m) and longer periods between collection times, sometimes resulting in postfire imagery collected several years after destruction had occurred and thus may have been more prone to undercounting destroyed buildings (*SI Appendix*, Supporting Text). However, annual destroyed building counts after 2002 were strongly correlated with counts from incident reports (26; r = 0.99; *SI Appendix*, Fig. S1). We found a significant increasing trend in annual building destruction rates, whether we used totals from incident reports or from our dataset (*SI Appendix*, Fig. S2).

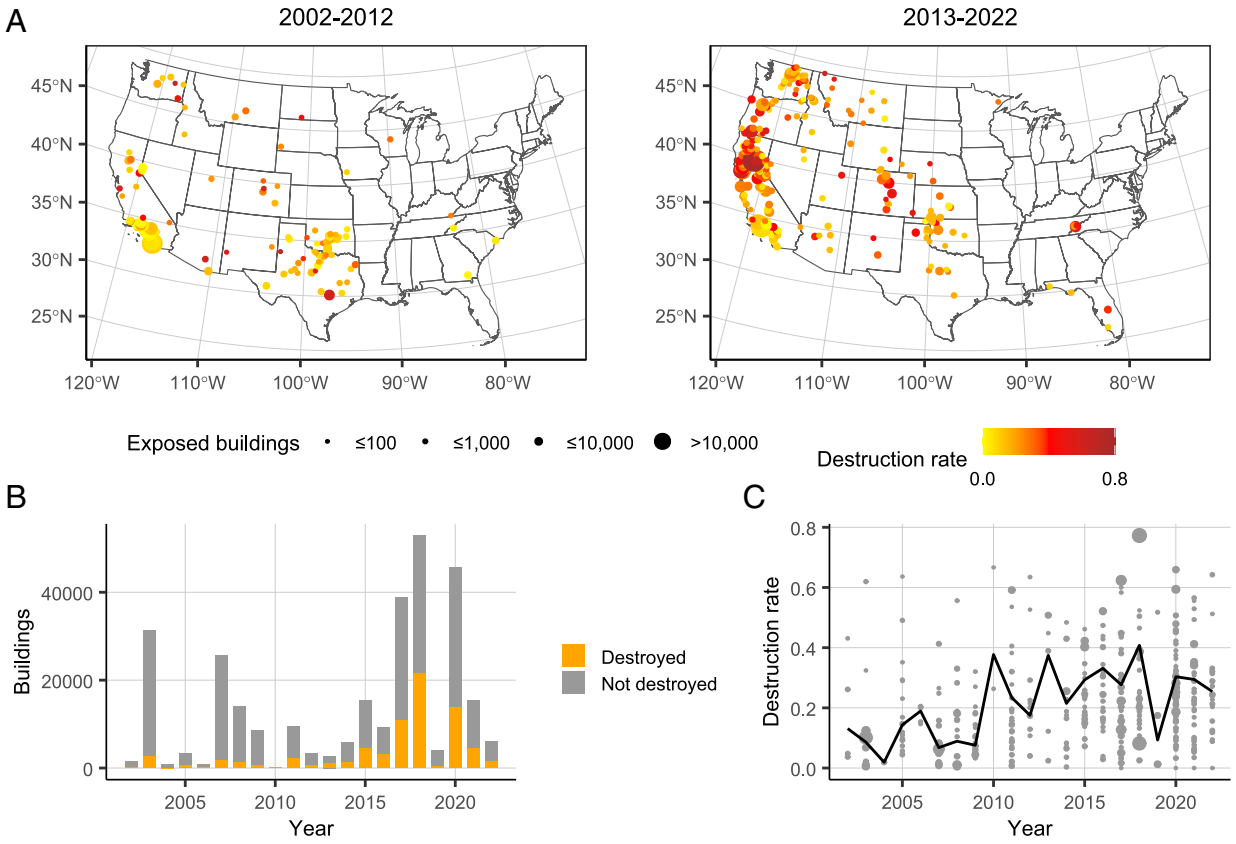

Fig. 1. (*A*) Wildfires that destroyed 10 or more buildings in the conterminous United States from 2002 to 2022, where we mapped all exposed and destroyed buildings. Point size indicates the number of exposed buildings and colors indicate the destruction rate, or number of buildings destroyed relative to number that was within or <100 m outside of the fire perimeter. (*B*) Numbers of buildings exposed to and destroyed by destructive wildfires by year. (*C*) Total annual destruction rate (line plot) and destruction rates for individual fire events (points) by year. Point size is proportional to number of exposed buildings.

More Building Exposure in Forests, But Increasing Destruction Rates in Other Vegetation Types. Trends in building exposure and destruction varied by ecoregions of the conterminous US. Annual numbers of buildings exposed to destructive wildfires increased most significantly from in the Western Forests ecoregion from 2002 to 2022, by a large magnitude (25%/year, relative to the 2002–2012 mean; p: 0.025; Table 1 and *SI Appendix*, Table S1). Increases in exposure were weakly significant in the Western Deserts (slope: 11.8%/year; p: 0.058) and Great Plains (slope: 7.8%/year; $P = 0.064$) but nonsignificant in Mediterranean California and the Eastern Forests ($P = 0.30$ and 0.12, respectively). Annual numbers of destroyed buildings increased significantly in the Western Forests, Western Deserts and Great Plains, but not in Mediterranean California or the Eastern Forests (Table 1 and Fig. 2 and *SI Appendix*, Table S1).

Destruction rates in the Western Forests ecoregion were substantially higher than in other western ecoregions (Table 1 and Fig. 2 and *SI Appendix*, Table S2). The Eastern Forests ecoregion also had high destruction rates (total: 36.9%) but had fewer buildings exposed to wildfire overall. However, destruction rates increased significantly over time in Mediterranean California, the Western Deserts, and the Great Plains ecoregions (Table 1 and Fig. 2).

In absolute numbers, most exposed and destroyed buildings were in grass and shrubland or evergreen forest (Table 2 and Fig. 3 *A* and *B*). The majority of exposed buildings were in grass and shrubland; however, there was a substantial increase in building exposure in evergreen forest (Fig. 3*A*). From 2002 to 2012, most destructive events occurred in southern California and the southern Great Plains (Fig. 1*A*), and 82.4% of exposed buildings were in grass and shrublands. From 2013 to 2022, the proportion of exposed buildings in grass and shrublands dropped to 61.3%, and the proportion in evergreen forests increased from 11.3% to 33.2%. Most notably, the majority of destroyed buildings from 2002 to 2012 were in grass and shrubland (62.2%), but from 2013 to 2022 this shifted to evergreen forest (50.1%).

Increases in building exposure in evergreen forests largely explain increasing destruction rates across the conterminous United States, as evergreen forests had consistently higher destruction rates than other vegetation types throughout our study period (Table 2 and Fig. 3*C*). Destruction rates were lowest in grass and shrublands (total: 16.6%). Buildings in evergreen forest were 3.4 times as likely to be destroyed as those in grass and shrublands, buildings in deciduous and mixed forest were 2.4 times as likely, and buildings in wetlands were 1.9 times as likely, after accounting for annual trends (*SI Appendix*, Table S3). These differences were not consistent over time, and destruction rates increased significantly in grass and shrublands and deciduous and mixed forests from 2002 to 2022 (Fig. 3*C* and Table 2). Only 2.4% of exposed buildings were in wetlands, and destruction rates for this vegetation type were highly variable (Fig. 3). Most fires where buildings were primarily in wetlands were in the southeastern coastal region or the northern forests; however, increases in the destruction rate for wetlands were strongly influenced by the 2020 Almeda Drive fire in western Oregon (Fig. 3 *B* and *C*).

Rising Destruction Rates Are Related to Changes in Vegetation Type, Fire Weather, and Development Type. The predictors that best explained wildfire destruction rates for building clusters were percentage of evergreen forest cover, mean energy release

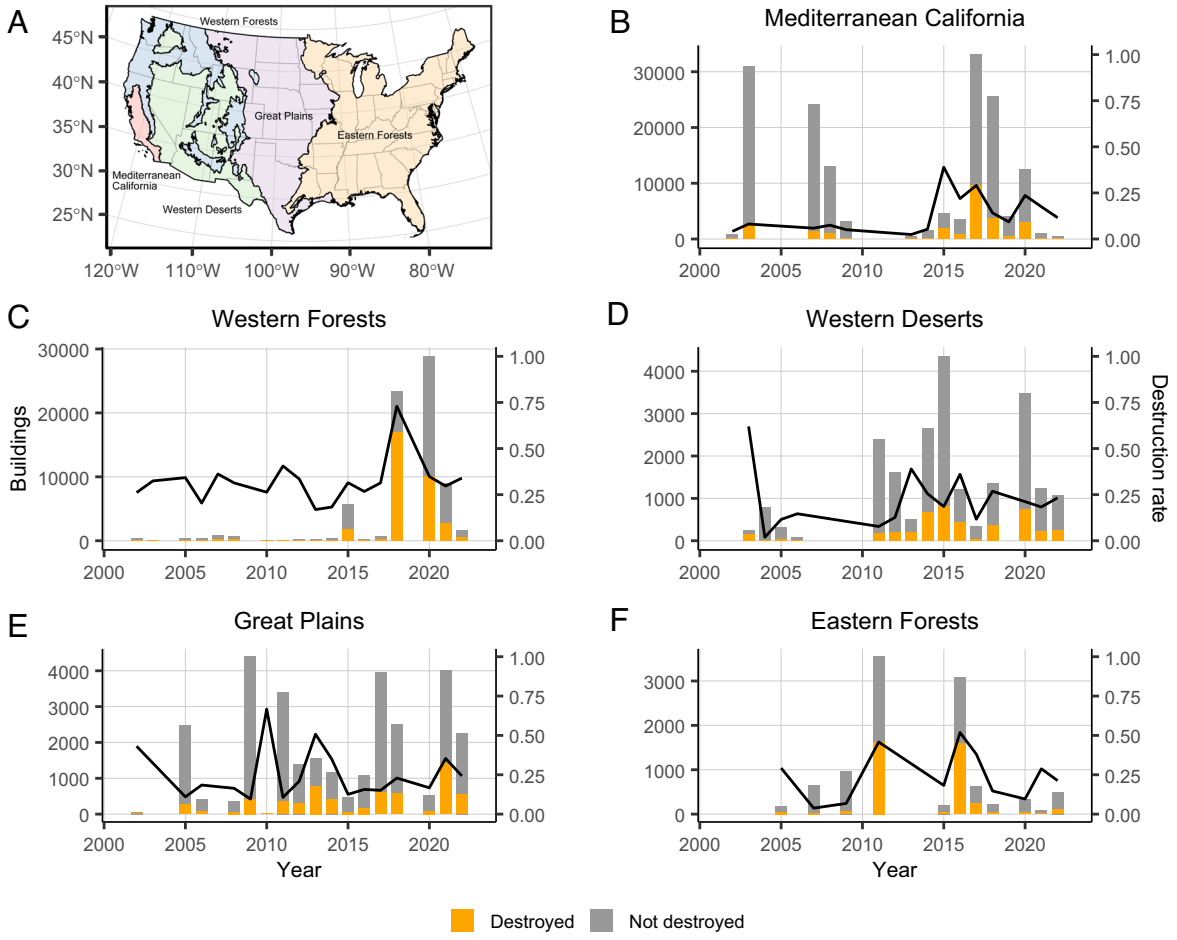

Fig. 2. (*A*) Major ecoregions in the conterminous United States, based on Level I ecoregions for North America (39). (*B*–*F*) Numbers of buildings exposed to and destroyed by destructive wildfires (bar charts) and total annual destruction rates (line plots) by year, by ecoregion.

component [ERC; a relative, unitless measure related to the heat released by burning, related to live and dead fuel moisture (41)] during the 7-d period following wildfire ignition, percentage of buildings in interface WUI, maximum wind speed, mean building distance to high-severity burned area, percentage of wetland cover, and percentage of buildings in low-density wildlands (*SI Appendix*, Tables S4–S6). Logistic regression models explained 80% of deviance and predicted reasonably well on test subsets (observed-predicted pseudo-R^2: 0.67; *SI Appendix*, Figs. S3 and S4). Destruction rates were positively correlated with evergreen forest and ERC in all ecoregions and negatively correlated with interface WUI in Mediterranean California, the Western Deserts, and the Great Plains (*SI Appendix*, Fig. S5). Very few exposed clusters had more than 20% interface WUI in the Western Forests and Eastern Forests, so it is unclear whether relationships are similar in these ecoregions. Destruction rates were positively correlated with maximum wind speed in Mediterranean California and the Eastern Forests but were only weakly correlated with wind speed in other ecoregions (*SI Appendix*, Fig. S5).

We tested how annual trends in wildfire building destruction rates were related to trends in fuels, weather, and WUI type by using our final logistic regression models to predict destruction rate response to each predictor, while holding all other predictors constant at their median values (Fig. 4). Our models predicted increases in annual destruction rates in response to 1) increases in the percentage of evergreen forest cover in proximity to exposed

Table 1. Trends in building destruction from destructive wildfires (≥10 destroyed buildings) in the conterminous United States, by major ecoregion, 2002–2022

Ecoregion	Exposed buildings trend (%/year)	Destroyed buildings trend (%/year)	Destruction rate trend (odds ratio/year)	Total destruction rate (%)
Mediterranean California	NS	NS	1.008 to 1.014	15.4
Western Forests	25.1*	20.7*	0.991 to 1.009	45.7
Western Deserts	11.8***	24.9*	1.003 to 1.010	20.0
Great Plains	7.8***	17.8*	1.007 to 1.012	20.5
Eastern Forests	NS	NS	1.000 to 1.021	36.9
All conterminous United States	5.8***	23.0**	1.014 to 1.018	24.6

Trends in numbers of exposed and destroyed buildings are relativized by their 2002–2012 means. Trend significance: **$P < 0.01$; *$P < 0.05$; ***$P < 0.1$; NS: nonsignificant. Odds ratios for destruction rate trends are based on logistic regression coefficients (odds ratio >1 indicates increasing trend, <1 indicates decreasing). Ranges indicate minimum and maximum coefficients, determined by fitting models leaving out one year of observations at a time to assess trend robustness.

Table 2. Destruction rates for buildings in each of four major vegetation types in the conterminous United States, 2002–2022

Vegetation type	Mean annual destruction rate ± std. dev. (%)	Relative destruction probability	Annual destruction rate trend (odds ratio/year)
Grass and shrubland	16.6 ± 9.2	1	1.010 to 1.013
Evergreen forest	33.6 ± 15.4	3.36	0.999 to 1.020
Deciduous/ mixed forest	25.8 ± 18.4	2.44	1.022 to 1.036
Wetland	12.2 ± 14.4	1.89	1.006 to 1.035

Relative destruction probability is based on factor intercepts of a logistic regression model, accounting for annual trends. Odds ratios for annual destruction rate trends are based on logistic regression coefficients (odds ratio >1 indicates increasing trend, <1 indicates decreasing). Ranges indicate minimum and maximum coefficients, determined by fitting models leaving out one year of observations at a time to assess trend robustness.

buildings, 2) increases in ERC, and 3) decreases in the percentage of exposed buildings in interface WUI (Fig. 4 and *SI Appendix*, Tables S7 and S8). Interface WUI had the largest effect size (0.41 ± 0.17 %/year), while evergreen forest and ERC had similar effect sizes (0.28 ± 0.09 %/year; 0.26 ± 0.08 %/year; respectively). There was no significant trend in response to maximum wind speed during wildfire events, although there was a significant increase in mean wind speed in the Western Forests, Western Deserts, and Great Plains (*SI Appendix*, Table S8). Our models did not indicate that increases in destruction rates were due to changes in the size of destructive wildfires or building proximity to high-severity burned areas (*SI Appendix*, Tables S7 and S8).

Discussion

Increasing wildfire building destruction in the conterminous United States from 2002 to 2022 was driven not only by wildfires exposing more buildings, due to increasing burned areas and growth of homes in the WUI, but by wildfires destroying exposed buildings at higher rates. Across the entire conterminous United States, this increase in building destruction rates was strongly related to increasing exposure in evergreen forests in the northwestern United States, where exposed buildings were much more likely to be destroyed than in other vegetation types. However, the majority of buildings that were exposed to wildfires from 2002 to 2022 were in grass and shrublands. Destruction rates significantly increased over time in grass and shrublands, as well as in deciduous and mixed forests. Our results indicate that the drivers of increasing wildfire destruction are varied and highlight challenges of adapting to dynamic wildfire risk.

Increasing burned areas in regions where wildfire was historically infrequent can lead to highly destructive events. In our analyses, this shift was most evident in the western Cascades region of Oregon, which experienced no destructive wildfires in 2002–2012 but experienced several highly destructive fires in September of 2020 in the midst of extreme high temperatures, drought, and winds (42). We found that destruction rates in this region were frequently above 50%, likely because dense forest fuels are prone to high-intensity fires and produce large numbers of embers (43). Wildfire in temperate and boreal forests has historically been limited by the occurrence of low-fuel moisture conditions, and warming in recent years has driven significant increases in fire size and frequency in these ecosystems globally (6). While destructive fires have occurred historically in this region, future projections indicate that the extreme conditions driving the 2020 fire season are

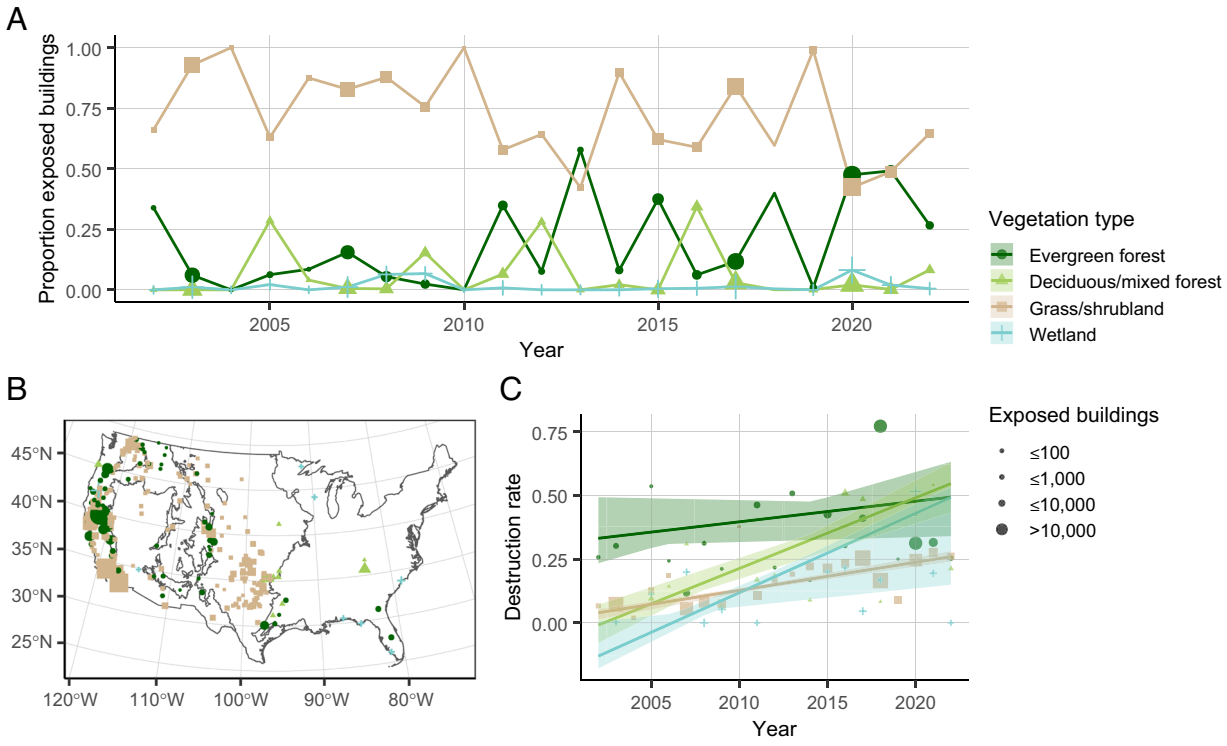

Fig. 3. (*A*) Proportions of buildings exposed to destructive wildfires (≥10 destroyed buildings) in different vegetation types in the conterminous United States, by year. (*B*) Locations of destructive wildfire events in the conterminous United States, with colors and symbols indicating the most common vegetation type within 1 km of exposed buildings. (*C*) Annual destruction rates for buildings in each vegetation type (point symbols) and linear trends (lines) based on logistic regression. The shaded area represents the range of predicted destruction rates using leave-one-out cross validation for individual years.

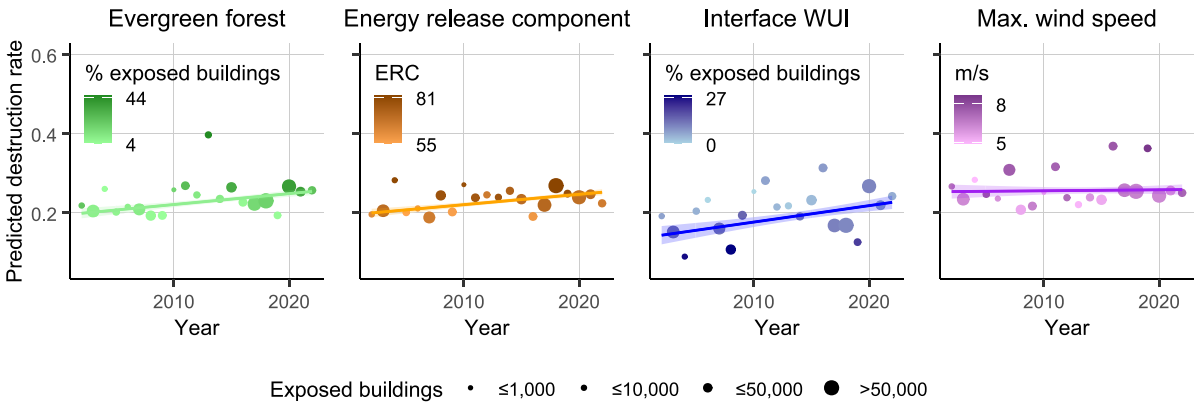

Fig. 4. Predicted annual building destruction rates for all wildfires in the conterminous United States in response to observed variation in each of the four top predictors in our logistic regression models, while holding all other predictors constant. Trendlines are based on logistic regressions weighted by numbers of exposed buildings in each fire, with shaded areas representing SE. Point colors are scaled to represent observed predictor values for all exposed buildings [% of exposed buildings where evergreen forest is the dominant vegetation type within 1 km; weighted mean of energy release component (ERC) by wildfire event; % of exposed buildings in interface WUI; weighted mean of maximum wind speed by wildfire event].

likely to occur more frequently in the Pacific Northwest over the 21st century (44).

Although much more burned area in the United States occurs in the western United States than in the east, the potential for increasing wildfire destruction in forested areas in the eastern United States is of concern because large populations live near forested WUI (11). The 8th most destructive fire in our dataset was Chimney Tops 2, which occurred in deciduous forest near Great Smoky Mountain National Park, near Gatlinburg, Tennessee, in 2016 and destroyed over 1,500 buildings (52.1% destruction rate). We did not observe a significant trend in numbers of exposed or destroyed buildings in the Eastern Forests and found that average ERC of destructive fires decreased over time, coincident with climate change-driven precipitation increases (45). However, it is highly uncertain how precipitation trends will continue and how warming temperatures will interact with precipitation to affect wildfire activity (46). Some regions of the southeastern United States have experienced increases in burned areas and wildfire size since the late 20th century, while burned areas have decreased in the north-central and northeastern United States (47). Growing burned areas in the southeast could lead to much greater home exposure, as parts of this region experienced more growth in the WUI than any other region in the United States in the 2010s (e.g., southeast Texas, the western Carolinas, and Florida; 11).

Outside of forests, many highly destructive wildfires occurred in Mediterranean-type shrublands in California, grasslands on the Rocky Mountain Front Range and southern Great Plains, and desert shrublands in the Great Basin (21). We found that increasing destruction rates in grass and shrubland-dominated ecoregions are linked to increasing ERC, which indicates lower fuel moisture and low-humidity conditions that can drive extreme fire behavior (41). Assessing relationships between climate and wildfire behavior is complex, however, because wildfire activity is linked not only to periods of low fuel moisture leading up to fire ignition, but to antecedent wet periods that allow for fuel buildup (48). Increasing "whiplash" between wet and dry extremes in the southwestern United States can create conditions for more extreme wildfire behavior (49), and the devastating Los Angeles fires in January 2025 provide an example of the high destruction that can occur during an extreme dry period that follows an extreme wet period, particularly during extreme high winds (50). Our study also did not assess how extreme fire behavior may have been exacerbated by the spread of flammable invasive grasses, which have altered fire frequency in the Great Basin, desert southwest, and southeastern pine savannahs (51).

Wildfire building destruction rates were influenced by development type as well as weather and wildland vegetation. In Mediterranean California, we found that increasing destruction rates were linked to a shift in exposure from interface WUI to low-density wildlands, as more destructive wildfires occurred in the northern California coastal mountains and Sierra Nevada foothills. Lower-density areas may face greater destruction likelihood as a result of lower suppression efforts, as they may have limited accessibility for firefighters or may be a lower priority for protection than higher-density areas where more buildings can be protected by focusing suppression efforts on a limited area (27, 29, 31). More dispersed buildings may also have more vegetation in the defensible space, increasing the likelihood of flame transmission and ignition (52). However, high-density developments may face high destruction risk when human-caused ignitions occur near communities during conditions that allow fires to spread rapidly, as these events can overwhelm suppression and turn into highly destructive urban conflagrations driven by home-to-home spread (16, 34). Home-hardening measures, such as building with flame-resistant materials and clearing defensible space, can significantly reduce the likelihood of building ignitions, thereby reducing the rate of building destruction (33, 53). Assessing these features for all fires included in our study was not feasible, but our results indicate that housing density and community layout relative to neighboring wildlands can mitigate wildfire risk.

Rising rates of wildfire building destruction compound the challenges of increasing wildfire exposure as burned areas continue to increase and as populations in the WUI continue to grow (54, 55). Vegetation management can reduce the potential for high-intensity wildfires near communities, while actions focused on reducing home susceptibility can help to minimize losses. Increasing building exposure and high destruction rates in forests suggest that forest fuel management can play an important role in risk reduction, with attention to the historical role of fire in different forested ecosystems. However, rising destruction rates in other ecosystem types indicate that policies other than forest thinning (e.g., invasive grass management, reducing ignitions caused by powerlines or other human activities, defensible space clearing, reducing exposure during new home construction) are also of importance. With all these potential management actions, resources and knowledge are needed for effective implementation.

Our study provides support for evidence-based risk management policies for preventing wildfire disasters.

Materials and Methods

Building Destruction Dataset. We created a dataset with point locations of all buildings that were exposed to destructive wildfires (≥10 buildings destroyed) in the conterminous United States from 2002 to 2022 (56; *SI Appendix*, Supporting Text). Buildings were mapped using high-resolution aerial and satellite imagery, using pre- and postfire imagery to manually assess building condition (destroyed or not destroyed). The dataset incorporated existing building destruction maps for 2002–2013 (29, 33; n = 124 fires) and for a few highly destructive events from 2014 to 2018 (34; n = 10 fires). We mapped all remaining fires that destroyed 10 or more buildings from 2014 to 2022 (n = 228), identified from final incident reports (40, 56). We used this threshold due to the time and labor constraints of manually classifying postfire building condition, which was necessary to achieve a suitable degree of accuracy across diverse landscapes with varying imagery quality, compared to automated classifications (57). We filtered the final dataset to include only fires where we were able to locate 10 or more major buildings (i.e., all permanent buildings approximately the size of a residential home or larger, excluding minor and mobile structures) that were destroyed.

Defining Building Exposure. Determining which buildings were exposed to wildfires is not straightforward because buildings can be ignited by embers at variable distances from the active flame front, depending on wind speed and ember production (58). Wildfire perimeter maps are typically drawn to include groups of destroyed buildings, and so only a small fraction of destroyed buildings in our dataset was outside of mapped fire perimeters (3.0%), even though some of these buildings may have been ignited by embers away from the flame front. The median distance for these buildings was 103 m (*SI Appendix*, Fig. S6). We therefore defined "directly" exposed buildings as all buildings that were inside fire perimeters or within 100 m of the perimeter. The 100 m buffer approximates the spatial uncertainty of perimeter maps based on 30-m Landsat pixels, the spatial uncertainty of building footprints, and defensible space around buildings (~30 m). This expanded definition included 98.4% of all destroyed buildings in our dataset. Although this approach does not perfectly account for all structures that face threats from wildfire, this provided a consistent definition that allowed us to assess temporal trends while accounting for most destroyed buildings.

We used our building dataset to assess spatial autocorrelation in destroyed buildings, to determine distances at which the likelihood of building destruction is influenced by neighboring buildings. We calculated correlograms for each fire and plotted means and SE of correlations at 100-m lag increments, up to 2,400 m. From this plot, we determined that autocorrelation diminished to <0.05 beyond distances of approx. 1,000 m (*SI Appendix*, Fig. S7). We therefore used this distance to summarize neighborhood variables around building points and to aggregate buildings into clusters.

Other Data. We defined major ecoregions for the conterminous United States based on the US Environmental Protection Agency's Level I ecoregions for North America (39) and defined major vegetation classes using National Land Cover Database annual products (NLCD; 59). Some Level I ecoregions had small extents within the conterminous United States, so we grouped these with larger ecoregions with similar vegetation types to define five major ecoregions (Fig. 2*A*). We grouped NLCD classes into four simplified vegetation classes (evergreen forests, deciduous and mixed forests, grass and shrublands, and wetlands; *SI Appendix*, Table S8). We calculated proportions of each class within 1 km of building points, based on the classification from the year prior to fire occurrence. We classified each building according to the class with the greatest proportion, excluding developed, agricultural, or other nonvegetated classes.

We determined WUI types using maps created by the SILVIS Lab at the University of Wisconsin–Madison, which are based on decadal census housing counts and NLCD vegetation cover (60). These maps classify census blocks into non-WUI, intermix WUI, or interface WUI according to minimum thresholds of housing density, wildland vegetation cover, and proximity to wildland vegetation based on US Federal Register definitions (38; *SI Appendix*, Table S9). We used these threshold classifications to identify intermix WUI (>6.17 houses/km^2, >50% vegetation cover) and interface WUI (>6.17 houses/km^2, <50% vegetation cover but within 2.4 km of a large vegetation patch). We then classified non-WUI blocks as "nonvegetated" (<50% vegetation cover) or "low-density wildlands" (>50% vegetation and <6.17 buildings/km^2).

Other predictor variables considered for inclusion in our logistic regression models were derived from 4-km gridded weather data (gridMET; 61), a 30-m digital elevation model (62), and burn severity and perimeter maps from MTBS (*SI Appendix*, Table S4). We selected mean and maximum wind speed and ERC as weather predictors because these variables predict fire spread and behavior (63). Due to the coarse resolution of weather data and uncertainty in dates when buildings were destroyed, we represented each weather variable as a single mean value for each wildfire event by extracting daily values for all pixels overlapping the fire perimeter, for the 7-d period including and following the date of ignition. We assessed burn severity by calculating distance from areas that were mapped in the "high" severity category by MTBS and extracted final fire size from MTBS perimeter maps. We used elevation data to calculate slope and aspect and transformed aspect to represent the absolute difference from southwest-facing (225°). We additionally used building point data to calculate building density within each fire perimeter, using a 1 km^2 window.

Trend Analysis. We assessed annual trends in the numbers of destroyed and exposed buildings and in predictor variables using Mann–Kendall tests with Theil–Sen slope estimators. We determined that there was no significant temporal autocorrelation in annual destruction rates and that our models were therefore appropriate for assessing annual trends (*SI Appendix*, Fig. S8). We assessed trends in annual destruction rates using logistic regression, weighted by the number of exposed buildings. For ecoregions, the response variable was destruction rate for individual fire events. For vegetation types, the response variable was the total annual destruction rate. We assessed trend robustness by sequentially fitting models with one year of observations excluded, then calculating means and ranges of slopes across all models. We exponentiated slopes to convert them to odds ratios, representing the increase or decrease in odds of destruction, given exposure, by year and among ecoregions or vegetation types.

Destruction Models. Past studies examining building loss within individual wildfires have found that building loss patterns exhibit strong spatial structure, reflecting the importance of home-to-home spread processes (29, 33). Furthermore, destruction likelihood for individual buildings is strongly predicted by building-level characteristics such as building age, materials, and vegetation within the defensible zone around homes (~30 m; 28, 29), which cannot be readily assessed at large scales for retrospective analysis. We therefore chose to model building destruction at an aggregated scale using clusters of adjacent buildings, similar to the approach used by Alexandre et al. (31). We defined clusters by grouping directly exposed buildings from individual fires with a maximum distance of 1 km, based on our spatial autocorrelation assessments.

We fit linear logistic regression models with cluster-level destruction rate as a binomial response, weighted by the number of exposed buildings. Models can be biased by including clusters with very few buildings, and so we fit models only using clusters with 10 or more destroyed buildings (n = 440). This retained 91% of exposed buildings (n = 268,885) and 97% of destroyed buildings (n = 70,158). For each cluster polygon, we extracted the percent cover of each major vegetation type based on the annual layer from the year prior to the fire, percent cover of each WUI type based on census block classifications from the year nearest the date of the fire (2000, 2010, or 2020), and means of building density, slope, transformed aspect, and distance to high-severity burned area. We also included final fire size, weather means, and year as predictors in our models. We fit univariate models for each predictor, then used a stepwise forward selection procedure in which we added variables that increased the total deviance explained (*SI Appendix*, Tables S5 and S6). We included ecoregion as a slope interaction for all model terms.

Data, Materials, and Software Availability. Geospatial data and CSV tables data have been deposited in USGS ScienceBase https://doi.org/10.5066/P1QX6UXD. The citation for the data release included in the manuscript is Carlson et al. (35).

ACKNOWLEDGMENTS. This work was funded by the National Land Imaging Program in the US Geological Survey Core Science Systems Mission Area and the Department of the Interior Office of Wildland Fire, applying funding under Section 40803 of the Bipartisan Infrastructure Law/Infrastructure Investment and Jobs Act through Intra-Departmental Agreement #IDG1000002441. We gratefully acknowledge the support by the Northern Research Station of the US Forest

Service, and by the Western Fire and Forest Resilience Collaborative via a grant from the John D. and Catherine T. MacArthur Foundation, the Gordon and Betty Moore Foundation (GBMF 11974 and 13283). We thank M. Hogan, B. Wittmer, Z. Ancona, and J. McBeth for digitizing work, M. Crist, S. Munson, D. Shinneman, and A. Russell for feedback on analyses, and J. Kreitler and two anonymous reviewers for providing comments on an early draft of this manuscript.

Author affiliations: [a]U.S. Geological Survey, Geosciences and Environmental Change Science Center, Denver, CO 80225; [b]U.S. Department of Agriculture Forest Service, Northern Research Station, Baltimore, MD 21228; [c]Dept. of Forest and Wildlife Ecology, University of Wisconsin-Madison, Madison, WI 53706; [d]U.S. Geological Survey, Southwest Biological Science Center, Flagstaff, AZ 86001; [e]U.S. Department of Agriculture Forest Service, Rocky Mountain Region, Fort Collins, CO 80526; [f]U.S. Geological Survey, Fort Collins Science Center, Fort Collins, CO 80526; [g]Dane County Land and Water Resources Department, Land Conservation Division, Madison, WI 53718; and [h]U.S. Geological Survey, Ecosystems Mission Area, Reston, VA 20192

Author contributions: A.R.C., T.J.H., M.H.M., V.C.R., L.S.B., J.R.M., and P.F.S. designed research; A.R.C., M.D.C., P.M.A., and H.A.K. performed research; A.R.C. analyzed data; T.J.H. conceptualized study, procured funding, supervised lead author and digitizers, oversaw analysis and reviewed manuscript; M.H.M., V.C.R., L.S.B., and J.R.M. reviewed early results, contributed to analysis questions, reviewed the paper and suggested edits; M.D.C. and H.A.K. contributed data, reviewed the paper and suggested edits; P.M.A. contributed data, reviewed paper and suggested edits; P.F.S. procured funding and supervised the development of project goals; and A.R.C. wrote the paper.

1. D. M. J. S. Bowman *et al.*, Human exposure and sensitivity to globally extreme wildfire events. *Nat. Ecol. Evol.* **1**, 0058 (2017).
2. P. E. Higuera *et al.*, Shifting social–ecological fire regimes explain increasing structure loss from Western wildfires. *PNAS Nexus* **2**, pgad005 (2023).
3. R. E. Munich, Wildfires and bushfires–Climate change increasing wildfire risk (2025), https://www.munichre.com/en/risks/natural-disasters/wildfires.html [Accessed 30 January 2025].
4. California Department of Insurance, Fact Sheet: Summary on Residential Insurance Policies and the FAIR Plan (2025).
5. A. Rosenthal, E. Stover, R. J. Haar, Health and social impacts of California wildfires and the deficiencies in current recovery resources: An exploratory qualitative study of systems-level issues. *PLoS One* **16**, e0248617 (2021).
6. M. W. Jones *et al.*, Global and regional trends and drivers of fire under climate change. *Rev. Geophys.* **60**, e2020RG000726 (2022).
7. W. M. Jolly *et al.*, Climate-induced variations in global wildfire danger from 1979 to 2013. *Nat. Commun.* **6**, 7537 (2015).
8. J. T. Abatzoglou, A. P. Williams, Impact of anthropogenic climate change on wildfire across western US forests. *PNAS* **113**, 11770–11775 (2016).
9. V. Iglesias, J. K. Balch, W. R. Travis, U.S. fires became larger, more frequent, and more widespread in the 2000s. *Sci. Adv.* **8**, eabc0020 (2022).
10. J. K. Balch *et al.*, Human-started wildfires expand the fire niche across the United States. *PNAS* **114**, 2946–2951 (2017).
11. V. C. Radeloff *et al.*, Rising wildfire risk to houses in the United States, especially in grasslands and shrublands. *Science* **382**, 702–707 (2023).
12. A. Modaresi Rad *et al.*, Human and infrastructure exposure to large wildfires in the United States. *Nat. Sustain.* **6**, 1343–1351 (2023).
13. M. R. Kreider *et al.*, Fire suppression makes wildfires more severe and accentuates impacts of climate change and fuel accumulation. *Nat. Commun.* **15**, 2412 (2024).
14. S. A. Parks *et al.*, A fire deficit persists across diverse North American forests despite recent increases in area burned. *Nat. Commun.* **16**, 1493 (2025).
15. W. R. L. Anderegg *et al.*, Tree mortality from drought, insects, and their interactions in a changing climate. *New Phytol.* **208**, 674–683 (2015).
16. J. K. Balch *et al.*, The fastest-growing and most destructive fires in the US (2001 to 2020). *Science* **386**, 425–431 (2024).
17. J. D. Coop, S. A. Parks, C. S. Stevens-Rumann, S. M. Ritter, C. M. Hoffman, Extreme fire spread events and area burned under recent and future climate in the western USA. *Glob. Ecol. Biogeogr.* **31**, 1949–1959 (2022).
18. S. Sachdeva, S. McCaffrey, Themes and patterns in print media coverage of wildfires in the USA, Canada and Australia: 1986–2016. *Int. J. Wildland Fire* **31**, 1089–1102 (2022).
19. U.S. House of Representatives, Fix our forests act (2025).
20. J. Salguero, J. Li, A. Farahmand, J. T. Reager, Wildfire trend analysis over the contiguous United States using remote sensing observations. *Remote Sens.* **12**, 2565 (2020).
21. J. T. Abatzoglou *et al.*, Downslope wind-driven fires in the western United States. *Earth's Future* **11**, e2022EF003471 (2023).
22. S. J. Prichard, N. A. Povak, M. C. Kennedy, D. W. Peterson, Fuel treatment effectiveness in the context of landform, vegetation, and large, wind-driven wildfires. *Ecol. Appl.* **30**, e02104 (2020).
23. J. B. Potts, S. L. Stephens, Invasive and native plant responses to shrubland fuel reduction: Comparing prescribed fire, mastication, and treatment season. *Biol. Conserv.* **142**, 1657–1664 (2009).
24. K. T. Davis *et al.*, Tamm review: A meta-analysis of thinning, prescribed fire, and wildfire effects on subsequent wildfire severity in conifer dominated forests of the Western US. *For. Ecol. Manage.* **561**, 121885 (2024).
25. M. R. Alizadeh *et al.*, Warming enabled upslope advance in western US forest fires. *Proc. Natl. Acad. Sci. U.S.A.* **118**, e2009717118 (2021).
26. J. E. Halofsky, D. L. Peterson, B. J. Harvey, Changing wildfire, changing forests: The effects of climate change on fire regimes and vegetation in the Pacific Northwest, USA. *Fire Ecol.* **16**, 4 (2020).
27. H. A. Kramer, M. H. Mockrin, P. M. Alexandre, V. C. Radeloff, High wildfire damage in interface communities in California. *Int. J. Wildland Fire* **28**, 641–650 (2019).
28. V. C. Radeloff *et al.*, The wildland-urban interface in the United States. *Ecol. Appl.* **15**, 799–805 (2005).
29. A. D. Syphard, J. E. Keeley, A. B. Massada, T. J. Brennan, V. C. Radeloff, Housing arrangement and location determine the likelihood of housing loss due to wildfire. *PLoS One* **7**, e33954 (2012).
30. C. A. Kolden, C. Henson, A socio-ecological approach to mitigating wildfire vulnerability in the wildland urban interface: A case study from the 2017 Thomas Fire. *Fire* **2**, 9 (2019).
31. P. M. Alexandre *et al.*, Factors related to building loss due to wildfires in the conterminous United States. *Ecol. Appl.* **26**, 2323–2338 (2016).
32. E. E. Knapp, Y. S. Valachovic, S. L. Quarles, N. G. Johnson, Housing arrangement and vegetation factors associated with single-family home survival in the 2018 Camp Fire. California. *Fire Ecol.* **17**, 25 (2021).
33. J. R. Meldrum *et al.*, Parcel-level risk affects wildfire outcomes: Insights from pre-fire rapid assessment data for homes destroyed in 2020 East Troublesome Fire. *Fire* **5**, 24 (2022).
34. D. E. Calkin *et al.*, Wildland-urban fire disasters aren't actually a wildfire problem. *Proc. Natl. Acad. Sci.* **120**, e2315797120 (2023).
35. A. Carlson *et al.*, Wildfire building destruction and exposure in the conterminous United States, 2002–2022. *USGS ScienceBase* (2025), 10.5066/P1QX6UXD, Deposited.
36. H. A. Kramer, M. H. Mockrin, P. M. Alexandre, S. I. Stewart, V. C. Radeloff, Where wildfires destroy buildings in the US relative to the wildland–urban interface and national fire outreach programs. *Int. J. Wildland Fire* **27**, 329–341 (2018).
37. M. D. Caggiano, T. J. Hawbaker, B. M. Gannon, C. M. Hoffman, Building loss in WUI disasters: Evaluating the core components of the wildland-urban interface definition. *Fire* **3**, 73 (2020).
38. U. S. Federal Register, Urban wildland interface communities within the vicinity of federal lands that are at high risk from wildfire (2001).
39. J. M. Omernik, Ecoregions of the conterminous United States. *Ann. Assoc. Am. Geogr.* **77**, 118–125 (1987).
40. L. A. St *et al.*, All-hazards dataset mined from the US National Incident Management System 1999–2014. *Sci. Data* **7**, 64 (2020).
41. J. E. Deeming, *The National Fire-Danger Rating System* (U.S. Department of Agriculture, Forest Service, Rocky Mountain Forest and Range Experiment Station, 1972).
42. J. T. Abatzoglou, D. E. Rupp, L. W. O'Neill, M. Sadegh, Compound extremes drive the Western Oregon wildfires of September 2020. *Geophys. Res. Lett.* **48**, e2021GL092520 (2021).
43. P. J. van Mantgem *et al.*, Climatic stress increases forest fire severity across the western United States. *Ecol. Lett.* **16**, 1151–1156 (2013).
44. D. E. Rupp *et al.*, Seasonal spatial patterns of projected anthropogenic warming in complex terrain: A modeling study of the western US. *Clim. Dyn.* **48**, 2191–2213 (2017).
45. H. Huang, C. M. Patricola, J. M. Winter, E. C. Osterberg, J. S. Mankin, Rise in Northeast US extreme precipitation caused by Atlantic variability and climate change. *Weather Clim. Extremes* **33**, 100351 (2021).
46. R. Barbero *et al.*, Multi-scalar influence of weather and climate on very large-fires in the eastern United States. *Int. J. Climatol.* **35**, 2180–2186 (2015).
47. V. M. Donovan, R. Crandall, J. Fill, C. L. Wonkka, Increasing large wildfire in the Eastern United States. *Geophys. Res. Lett.* **50**, e2023GL107051 (2023).
48. J. E. Keeley, Impact of antecedent climate on fire regimes in coastal California*. *Int. J. Wildland Fire* **13**, 173–182 (2004).
49. D. Swain *et al.*, Increasing hydroclimatic whiplash can amplify wildfire risk in a warming climate. *Glob. Change Biol.* **31**, e70075 (2025).
50. T. Brown, J. Shelton, Confluence of fire and people. *Nat. Sustain.* **8**, 329–330 (2025).
51. E. J. Fusco, J. T. Finn, J. K. Balch, R. C. Nagy, B. A. Bradley, Invasive grasses increase fire occurrence and frequency across US ecoregions. *PNAS* **116**, 23594–23599 (2019).
52. S. E. Caton, R. S. P. Hakes, D. J. Gorham, A. Zhou, M. J. Gollner, Review of pathways for building fire spread in the wildland urban interface part I: Exposure conditions. *Fire Technol.* **53**, 429–473 (2017).
53. T. D. Penman *et al.*, Reducing the risk of house loss due to wildfires. *Environ. Model. Softw.* **67**, 12–25 (2015).
54. C. Burton *et al.*, Global burned area increasingly explained by climate change. *Nat. Clim. Chang.* **14**, 1186–1192 (2024), 10.1038/s41558-024-02140-w.
55. F. Schug *et al.*, The global wildland–urban interface. *Nature* **621**, 94–99 (2023).
56. National Wildfire Coordinating Group, SIT/209-HISTORICAL. FAMWeb Data Warehouse. (2025), Deposited.
57. N. K. Kasraee, T. J. Hawbaker, V. C. Radeloff, Identifying building locations in the wildland–urban interface before and after fires with convolutional neural networks. *Int. J. Wildland Fire* **32**, 610–621 (2023).
58. M. E. Roberts, A. A. Rawlinson, Z. Wang, Ember risk modelling for improved wildfire risk management in the peri-urban fringes. *Environ. Model. Softw.* **138**, 104956 (2021).
59. U. S. Geological Survey, Annual NLCD Collection 1 Science Products. *USGS ScienceBase* (2024), https://doi.org/10.5066/P94UXNTS, [Deposited 2024].
60. V. C. Radeloff *et al.*, The 1990–2020 wildland-urban interface of the conterminous United States–geospatial data. *Forest Service Research Data Archive*, ed. 4 (2023), https://doi.org/10.2737/RDS-2015-0012-4, [Deposited 2023].
61. J. T. Abatzoglou, Development of gridded surface meteorological data for ecological applications and modelling. *Int. J. Climatol.* **33**, 121–131 (2013).
62. USGS 3D Elevation Program, 1 Arc-second Digital Elevation Models (DEMs)–USGS National Map 3DEP Downloadable Data Collection. *USGS ScienceBase* (2024) [Deposited 2024].
63. M. A. Finney, S. S. McAllister, T. P. Grumstrup, J. M. Forthofer, *Wildland Fire Behavior: Dynamics, Principles and Processes* (CSIRO Publishing, 2021).